

Article

Unexpected Findings in 16th Century Wall Paintings: Identification of Aragonite and Unusual Pigments

Laura Rampazzi ^{1,2,*} , Cristina Corti ³ , Ludovico Geminiani ³  and Sandro Recchia ³

¹ Dipartimento di Scienze Umane e dell'Innovazione per il Territorio e Centro Speciale di Scienze e Simbolica dei Beni Culturali, Università degli Studi dell'Insubria, via Valleggio 9, 22100 Como, Italy

² Istituto per le Scienze del Patrimonio Culturale, Consiglio Nazionale delle Ricerche (ISPC-CNR), via Cozzi 53, 20125 Milano, Italy

³ Dipartimento di Scienza e Alta Tecnologia, Università degli Studi dell'Insubria, via Valleggio 11, 22100 Como, Italy; cristina.corti@uninsubria.it (C.C.); lgeminiani@studenti.uninsubria.it (L.G.); sandro.recchia@uninsubria.it (S.R.)

* Correspondence: laura.rampazzi@uninsubria.it

Abstract: Sixteenth century wall paintings were analyzed from a church in an advanced state of decay in the Apennines of central Italy, now a remote area but once located along the salt routes from the Po Valley to the Ligurian Sea. Infrared spectroscopy (FTIR-ATR), X-ray diffraction (XRD) and scanning electron microscopy (SEM) with a microprobe were used to identify the painting materials, as input for possible future restoration. Together with the pigments traditionally used for wall painting, such as ochre, ultramarine blue, bianco di Sangiovanni, cinnabar/vermilion, azurite, some colors were also found to have only been used since the 18th century. This thus suggests that a series of decorative cycles occurred after the church was built, confirmed by the multilayer stratigraphy of the fragments. Some of these colors were also unusual, such as clinocllore, Brunswick green, and ultramarine yellow. The most notable result of the analytical campaign however, was the ubiquitous determination of aragonite, the mineralogical form of calcium carbonate, mainly of biogenic origin. Sources report its use in Roman times as an aggregate in mortars, and in the literature it has only been shown in Roman wall paintings. Its use in 16th century wall paintings is thus surprising.

Keywords: aragonite; Brunswick green; clinocllore; FTIR; mortars; SEM-EDX; ultramarine yellow; vermilion; wall paintings; XRD



Citation: Rampazzi, L.; Corti, C.; Geminiani, L.; Recchia, S. Unexpected Findings in 16th Century Wall Paintings: Identification of Aragonite and Unusual Pigments. *Heritage* **2021**, *4*, 2431–2448. <https://doi.org/10.3390/heritage4030137>

Academic Editor: Diego Tamburini

Received: 30 August 2021

Accepted: 12 September 2021

Published: 15 September 2021

Publisher's Note: MDPI stays neutral with regard to jurisdictional claims in published maps and institutional affiliations.



Copyright: © 2021 by the authors. Licensee MDPI, Basel, Switzerland. This article is an open access article distributed under the terms and conditions of the Creative Commons Attribution (CC BY) license (<https://creativecommons.org/licenses/by/4.0/>).

1. Introduction

Conservation science helps preserve the memory of monuments which have been shown to be in such a declining state of neglect and decay that time is running out. Monuments that very probably cannot be restored as part of a conservation project risk disappearing without a trace. An analytical campaign of what is still possible to characterize can therefore reveal the materials, artistic techniques, decorations to future memory of a disappearing beauty. The church of Santo Stefano in Selva (Cerignale) (Figure 1), in the Apennines of Piacenza (central Italy), is in a declining state of neglect and decay. Given its location in a remote area, with no tourism, it is not a high priority for the national heritage. The local community pressed for an analytical campaign on the fragments of the few surviving paintings, in order to preserve their memory.

The area between the Po Valley and the Ligurian Sea was once much travelled, and there were also several historical pilgrimages, along important trade ridgeways, such as the salt routes, which involved the exchange of local goods. One of these routes, the “Strada del Cifalco”, followed the natural path of the Trebbia Valley along the ridge between the Aveto and Trebbia rivers, connecting the north of what today is Liguria with Piacenza. It is thus not surprising that the Apennines, the mountainous system of this area, are rich in artistic testimonies, which unfortunately were neglected during the depopulation after

the Second World War. This artistic history can be seen in the municipality of Cerignale too: the village of Ponte Organasco, with its medieval layout and many tower houses; the medieval castle of Cariseto, which hosted Emperor Frederick Barbarossa; and the church of Santo Stefano in Selva. The building is located in an area which was once a point of transit and rest for the muleteers travelling between the Trebbia valley and the Aveto valley, on their way to Liguria [1].



Figure 1. The remains of wall paintings in the church of S. Stefano.

Documentation on the history of the paintings is scarce. The building is listed in a church register which records the churches that in 1523 sent financial dues to the Papal State. The ruins still reveal the elaborate construction technique adopted to simulate a certain opulence, such as the vaulted ceiling, which looks like it is made of stone, but is actually a wooden structure with the intrados made of reeds covered with painted plaster. The facade of the single-nave church is relatively intact, and recalls the classical Greek temple structure. The lesenes support the very elaborate trabeation and triangular tympanum. Three transverse round arches have also remained intact. No records of the wall paintings have been found in the archives. We can thus only assume that the first cycle of paintings dates back to the construction of the building in the 16th century.

The church has almost completely lost the internal wall paintings (Figure 1). The decay originated from the partial settlement of the ground, around the middle of the last century, and more recently from a bolt of lightning that hit the stone bell tower causing a fire that almost completely destroyed the roof.

The present work reports the analytical campaign conducted on fragments from the few wall paintings still in place. The samples were analyzed with optical microscopy and scanning electron microscopy equipped with an energy-dispersive spectrometer, also on polished cross sections, and with X-ray diffraction and infrared spectroscopy on powders. The analyses obtained important information on the pictorial materials, pigments and

binders used for the decoration of the walls. Traditional and unusual pigments were revealed together with the widespread use of aragonite probably from shells utilized as a building material, which, to the best of our knowledge, has never before been found in 16th century wall paintings.

We believe that the results could contribute to maintain the memory of the history of the church and help support a material study as part of future conservation work.

2. Materials and Methods

Table 1 reports the samples. Since most of the samples had clearly different overlapping color backgrounds, when possible without risk of contamination, the individual layers were separated with a scalpel and analyzed individually. Fragments of the eight most complex samples were analyzed as polished cross sections. From each fragment, the support mortar layer was taken and characterized.

Table 1. Description of the samples, identified pigments and employed analytical techniques (OM: optical microscopy; FTIR-ATR: Fourier-transform infrared spectroscopy in attenuated total reflection; XRD: X-ray diffraction; SEM-EDX: scanning electron microscopy-energy dispersive X-ray spectroscopy; PCS: polished cross section).

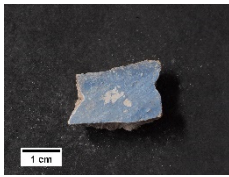
Sample	Images	Colors	Identified Pigments	Analytical Techniques
ST1		aqua green	blanc fixe (BaSO ₄), clinochlore (Mg ₄ Fe ₂ Al(Si ₃ Al)O ₁₀ (OH) ₈), ultramarine blue (Na ₈ Al ₆ Si ₆ O ₂₄ S ₄)	OM, FTIR-ATR, XRD, SEM-EDX
ST2		aqua green	blanc fixe (BaSO ₄), ultramarine blue (Na ₈ Al ₆ Si ₆ O ₂₄ S ₄)	FTIR-ATR, XRD, SEM-EDX, PCS
		blue	ultramarine blue (Na ₈ Al ₆ Si ₆ O ₂₄ S ₄)	
		red	red ochre (Fe ₂ O ₃ , clay)	
		white	blanc fixe (BaSO ₄)	
		yellow	yellow ochre (FeOOH, clay)	
ST3		aqua green	ultramarine blue (Na ₈ Al ₆ Si ₆ O ₂₄ S ₄), ultramarine yellow (BaCrO ₄)	FTIR-ATR, SEM-EDX, PCS
		blue	ultramarine blue (Na ₈ Al ₆ Si ₆ O ₂₄ S ₄)	
		white	bianco di Sangiovanni (CaCO ₃)	
		yellow	yellow ochre (FeOOH, clay)	
ST4		blue	ultramarine blue (Na ₈ Al ₆ Si ₆ O ₂₄ S ₄)	FTIR-ATR, XRD, SEM-EDX

Table 1. Cont.

Sample	Images	Colors	Identified Pigments	Analytical Techniques
ST5		blue	ultramarine blue ($\text{Na}_8\text{Al}_6\text{Si}_6\text{O}_{24}\text{S}_4$)	OM, FTIR-ATR, XRD, SEM-EDX, PCS
		red	red ochre (Fe_2O_3 , clay)	
		white	bianco di Sangiovanni (CaCO_3)	
ST6		blue	ultramarine blue ($\text{Na}_8\text{Al}_6\text{Si}_6\text{O}_{24}\text{S}_4$)	FTIR-ATR, XRD, SEM-EDX
		red	red ochre (Fe_2O_3 , clay)	
		yellow	cinnabar/vermilion (HgS), yellow ochre (FeOOH , clay)	
ST7		black	red ochre (Fe_2O_3 , clay)	OM, FTIR-ATR, SEM-EDX
		blue	blanc fixe (BaSO_4), ultramarine blue ($\text{Na}_8\text{Al}_6\text{Si}_6\text{O}_{24}\text{S}_4$)	
		light blue	blanc fixe (BaSO_4), ultramarine blue ($\text{Na}_8\text{Al}_6\text{Si}_6\text{O}_{24}\text{S}_4$), white lead (2PbCO_3 , $\text{Pb}(\text{OH})_2$)	
		grey	manganese black (MnO_2), yellow ochre (FeOOH , clay)	
		dark ochre	manganese black (MnO_2), yellow ochre (FeOOH , clay)	
		yellow	yellow ochre (FeOOH , clay)	
ST8		green	Brunswick green ($(\text{Cu,Zn})_2(\text{OH})_3\text{Cl}$)	OM, FTIR-ATR, XRD, SEM-EDX
		orange	yellow ochre (FeOOH , clay)	
		yellow	chrome yellow (PbCrO_4)	
ST9		ochre	yellow ochre (FeOOH , clay)	FTIR-ATR, SEM-EDX
ST10		red	red ochre (Fe_2O_3 , clay)	OM, FTIR-ATR, SEM-EDX
		yellow	yellow ochre (FeOOH , clay)	
ST11		green	Brunswick green ($(\text{Cu,Zn})_2(\text{OH})_3\text{Cl}$)	OM, FTIR-ATR, XRD, SEM-EDX
		yellow	chrome yellow (PbCrO_4), yellow ochre (FeOOH , clay)	

Table 1. Cont.

Sample	Images	Colors	Identified Pigments	Analytical Techniques
ST12		red	cinnabar/vermilion (HgS)	FTIR-ATR, SEM-EDX
		yellow	chrome yellow (PbCrO ₄), yellow ochre (FeOOH, clay)	
ST13		red	cinnabar/vermilion (HgS), yellow ochre (FeOOH, clay)	FTIR-ATR, SEM-EDX
		yellow	chrome yellow (PbCrO ₄), ultramarine yellow (BaCrO ₄)	
ST14		blue	ultramarine blue (Na ₈ Al ₆ Si ₆ O ₂₄ S ₄)	FTIR-ATR, SEM-EDX, PCS
		red	cinnabar/vermilion (HgS), red ochre (Fe ₂ O ₃ , clay)	
		white	bianco di Sangiovanni (CaCO ₃)	
		yellow	chrome yellow (PbCrO ₄), yellow ochre (FeOOH, clay)	
ST15		red	cinnabar/vermilion (HgS), red ochre (Fe ₂ O ₃ , clay)	OM, FTIR-ATR, SEM-EDX
		light red	blanc fixe (BaSO ₄), red ochre (Fe ₂ O ₃ , clay)	
		white	bianco di Sangiovanni (CaCO ₃)	
		yellow	chrome yellow (PbCrO ₄), yellow ochre (FeOOH, clay)	
ST16		light blue	ultramarine blue (Na ₈ Al ₆ Si ₆ O ₂₄ S ₄)	OM, FTIR-ATR, SEM-EDX
		red	cinnabar/vermilion (HgS), red ochre (Fe ₂ O ₃ , clay)	
		light red	red ochre (Fe ₂ O ₃ , clay)	
		yellow	chrome yellow (PbCrO ₄)	
ST17		blue	ultramarine blue (Na ₈ Al ₆ Si ₆ O ₂₄ S ₄)	OM, FTIR-ATR, SEM-EDX, PCS
		dark red	red ochre (Fe ₂ O ₃ , clay)	
		light red	red ochre (Fe ₂ O ₃ , clay)	
		white	bianco di Sangiovanni (CaCO ₃)	
ST18		blue	ultramarine blue (Na ₈ Al ₆ Si ₆ O ₂₄ S ₄)	OM, FTIR-ATR, XRD, SEM-EDX, PCS
		light blue	ultramarine blue (Na ₈ Al ₆ Si ₆ O ₂₄ S ₄)	
		red	red ochre (Fe ₂ O ₃ , clay)	
		yellow	yellow ochre (FeOOH, clay)	

Table 1. Cont.

Sample	Images	Colors	Identified Pigments	Analytical Techniques
ST19		blue	ultramarine blue ($\text{Na}_8\text{Al}_6\text{Si}_6\text{O}_{24}\text{S}_4$)	OM, FTIR-ATR, SEM-EDX, PCS
		light blue	azurite ($2\text{CuCO}_3 \cdot \text{Cu}(\text{OH})_2$)	
		dark ochre	yellow ochre (FeOOH , clay)	
		red	red ochre (Fe_2O_3 , clay)	
ST20		blue	ultramarine blue ($\text{Na}_8\text{Al}_6\text{Si}_6\text{O}_{24}\text{S}_4$)	OM, FTIR-ATR, SEM-EDX, PCS
		red	cinnabar/vermillion (HgS), red ochre (Fe_2O_3 , clay)	
		white	bianco di Sangiovanni (CaCO_3)	
		yellow	chrome yellow (PbCrO_4), yellow ochre (FeOOH , clay)	
ST21		light blue	ultramarine blue ($\text{Na}_8\text{Al}_6\text{Si}_6\text{O}_{24}\text{S}_4$)	OM, FTIR-ATR, SEM-EDX
		red	red ochre (Fe_2O_3 , clay)	
		white	bianco di Sangiovanni (CaCO_3)	
		yellow	yellow ochre (FeOOH , clay)	
ST22		light blue	ultramarine blue ($\text{Na}_8\text{Al}_6\text{Si}_6\text{O}_{24}\text{S}_4$)	OM, FTIR-ATR, SEM-EDX
		red	red ochre (Fe_2O_3 , clay)	
		yellow	yellow ochre (FeOOH , clay)	
ST23		red	yellow ochre (FeOOH , clay)	OM, FTIR-ATR, SEM-EDX
		yellow	red ochre (Fe_2O_3 , clay)	

2.1. Sampling

Samples were collected from detached fragments of wall paintings and stored in LDPE bags or containers.

2.2. Infrared Spectroscopy

FTIR-ATR spectra were acquired by means of a Thermo Scientific Nicolet iS10 instrument, in the range between 4000 and 600 cm^{-1} , 4 cm^{-1} resolution, 32 scans. The background was periodically registered. Spectra were interpreted by comparison with a homemade reference database and with the literature.

2.3. X-ray Diffraction

A selection of samples was analyzed as fine ground powders. X-ray diffraction analyses were performed using a Rigaku Miniflex 300 diffractometer (30 kV , 10 mA , $\text{Cu-K}\alpha$ radiation ($\lambda = 1.5418\text{ \AA}$), $5\text{--}55^\circ$ Theta/2-Theta, step scan 0.02° , scan speed $3^\circ/\text{min}$). PDXL2 software supporting ICDD (The International Centre for Diffraction Data) PDF2 databases were used to identify the phases.

2.4. Scanning Electron Microscopy and Energy Dispersive X-ray Spectroscopy

The samples were observed without any pre-treatment with a FEI/Philips XL30 ESEM (low vacuum mode—1 torr, 20 kV, BSE detector). The possibility of working in “low vacuum mode” made it possible not to cover the samples with a conductive layer of carbon or gold. Depending on the size of the collected fragments, they were either observed whole or broken up to obtain a significant portion that was compatible with the size of the sample holder. The elemental analyses were carried out using an X-ray energy dispersive spectrometer, EDAX AMETEK Element, coupled to SEM.

A selection of fragments was also embedded in an epoxy resin, cross-cut with a diamond saw and then mechanically polished. Polished cross sections were then analyzed by SEM-EDX, too.

2.5. Optical Microscopy

Samples were observed with an optical microscope Nikon Eclipse LV150, equipped with a Nikon DS-FI1 digital image acquisition system. Images were acquired and elaborated using the NIS-elements F software. Polished cross sections were observed with a portable digital microscope MAOZUA USB001, and images were acquired using the software MicroCapture Plus.

3. Results

The fragments analyzed had different colored layers that were identified by IR spectra and XRD analysis of the powders or suggested by EDX elemental spectra and maps (Table 1).

Yellow and red ochre were identified based on XRD and FTIR patterns, and then confirmed by iron associated with silicon and aluminum in EDX maps. For example, the FTIR spectrum (Figure 2a) of the yellow areas of sample ST7 showed peaks at 3150 and 798 cm^{-1} , which could be attributed to OH stretching and out-of-plane deformation of goethite, respectively; the pattern presented signals at 3691, 3649 and 3619 and 912 cm^{-1} too, which resemble the outer and inner OH group stretching and deformation of kaolinite, respectively [2–4]. The signals at 1027 (Si-O-Si), 1004 (Si-O-Al) and 938 cm^{-1} (Al-O-H) confirm our findings. Kaolinite is normally associated with the presence of ochre [5]. The absorbance at 1162 cm^{-1} (Si-O asymmetric stretching) is due to the presence of quartz, as well as the peak at 691 cm^{-1} which is Si-O symmetric stretching mode [2,3].

The powders of sample ST1, which is colored in aqua green, were analyzed with XRD (Figure 3). A comparison with the instrument database revealed the presence of clinocllore ($\text{Mg}_3(\text{Mg}_2\text{Al})(\text{Si}_3\text{Al})\text{O}_{10}$), which is a member of the chlorite group, with a color that varies between yellowish green, olive green, blackish green and bluish green [6]. The characteristic peaks of calcite (CaCO_3), gypsum ($\text{CaSO}_4 \cdot 2\text{H}_2\text{O}$), bassanite ($\text{CaSO}_4 \cdot 0.5\text{H}_2\text{O}$), quartz (SiO_2) and barite (BaSO_4) were also observed.

The pattern of IR bands (Figure 4a) at around 1410 cm^{-1} (C-O asymmetric stretching) and 1793 cm^{-1} (combination band), 873 and 712 cm^{-1} (C-O out-of-plane and in-plane bending vibrations, respectively) is present in all the spectra, which suggests the presence of calcium carbonate as calcite from the binder fraction of the mortar substrate [7–12]. The spectra of the white areas present only the peaks at around 1793, 1410, 873 and 712 cm^{-1} , which, as just discussed, refer to calcium carbonate, which constitutes the pigment bianco di Sangiovanni [6].

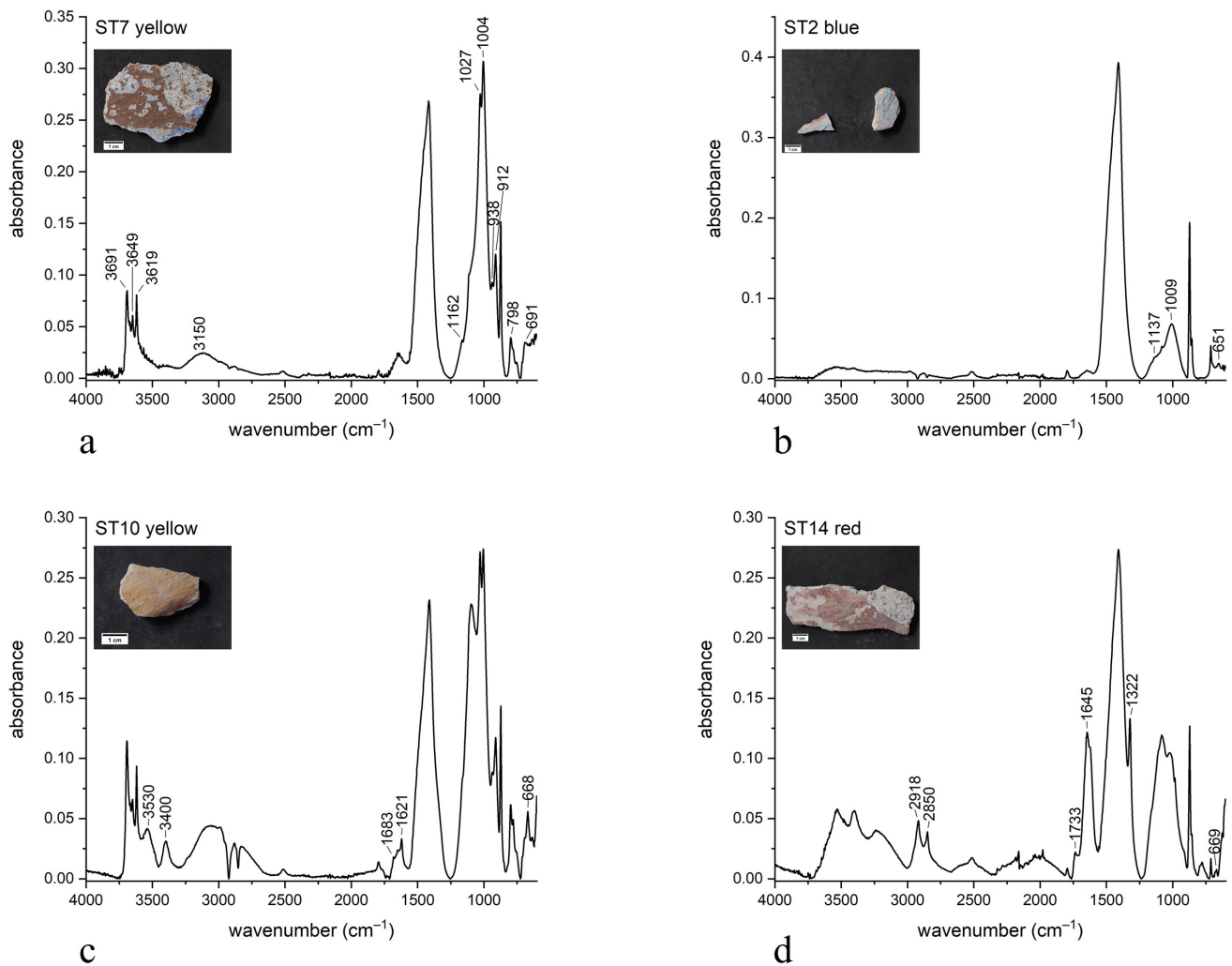


Figure 2. ATR spectra of: (a) yellow area of sample ST7, showing the presence of kaolinite, goethite and calcite; (b) blue area of sample ST2, showing the presence of ultramarine blue, calcite, aragonite; (c) yellow area of sample ST10, showing the presence of gypsum, calcite, ochre, traces of organic compounds; (d) red area of sample ST14, showing the presence of calcium oxalate, calcite, ochre, organic compounds.

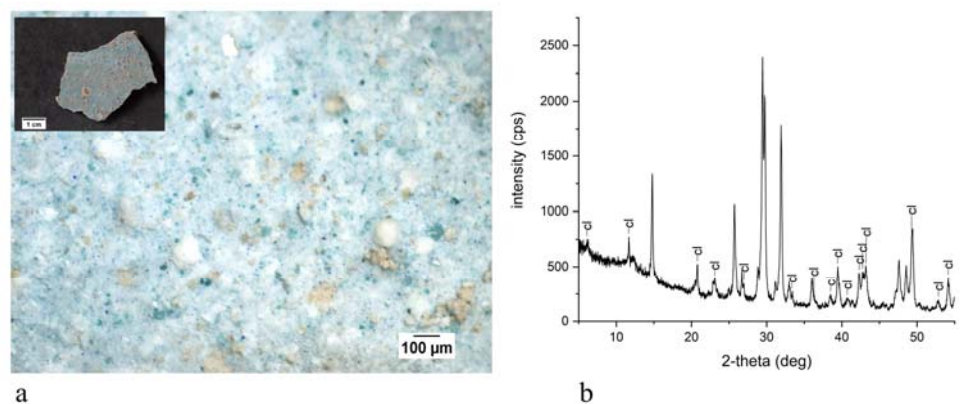


Figure 3. Aqua green area of sample ST1: digital microscope image of the surface (a) and XRD analysis on powders (b) showing the main signals of clinocllore (c).

The specific peaks at around 1083, 855 and 702 cm^{-1} found in all the samples suggest the presence of calcium carbonate in the mineralogical form of aragonite, both in the

support and mixed with the pigments. The 855 and 702 cm^{-1} signals are due to ν_2 and ν_4 CO_3^{2-} vibrations, respectively, and the absorbance at 1083 cm^{-1} could be attributed to ν_1 symmetric CO_3^{2-} stretching [13,14]. Figure 4a shows a representative spectrum of aragonite, identified in sample ST6, where the peaks are clearly distinguished from those of calcite. SEM images of sample ST19 (Figure 4b) clearly showed the typical sharp, needle-like crystals of aragonite [15]. Aragonite was always corroborated by the XRD pattern, which also distinguished between the two mineralogical forms of calcium carbonate (Figure 4c).

In some red samples, the EDX investigations showed the distribution of mercury and sulfur in the same area, suggesting the use of cinnabar/vermilion, as in sample ST15 (Figure 5). Similarly, the co-presence of chrome and lead in EDX maps indicated the presence of chrome yellow, as in the yellow area in sample ST11, where the pigment was confirmed by the signals of crocoite (PbCrO_4) present in XRD results (Figure 6).

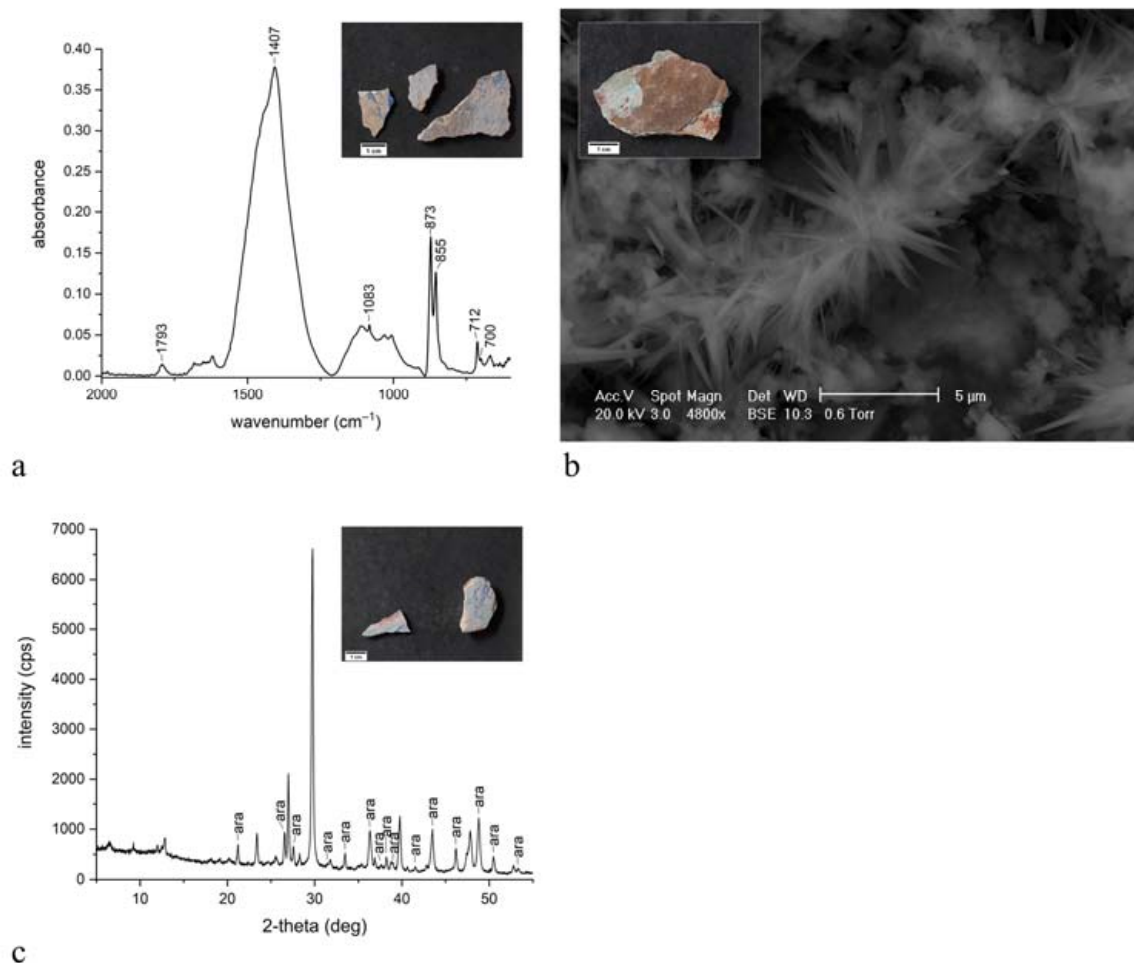


Figure 4. (a) ATR spectra of the red area of sample ST6, showing the peaks of calcite, aragonite, ochre; (b) SEM image in BSE mode of the surface of sample ST19: the typical sharp crystals of aragonite are shown; (c) XRD analysis on powders of mortar support of sample ST2, showing the main signals of aragonite (ara).

The spectrum of the blue areas showed peaks at 1137, 1009 and 651 cm^{-1} , which could be attributed to Si-O-Si and Si-O-Al stretching modes of ultramarine blue ($\text{Na}_8\text{Al}_6\text{Si}_6\text{O}_{24}\text{S}_4$), respectively [16]. Figure 2b shows a spectrum of ultramarine, as found in sample ST2.

Blanc fixe (barium sulphate BaSO_4) was found in some samples due to the presence of IR peaks at 3606, 1089 and 659 cm^{-1} , which can be attributed to OH (surface-adsorbed water molecules), SO_4^{2-} and Ba-S-O stretching modes, respectively [17]. EDX maps of sulfur and barium and XRD patterns of barite recorded in the same areas corroborated the hypothesis.

Gypsum was present in most samples, as highlighted by the XRD results and by the IR signals (Figure 2c) at around 3530 and 3400 (hydroxyl stretching bands), 1683 and 1621 (hydroxyl bending vibrations), 1113 (SO asymmetric stretching), and 668 cm^{-1} (SO asymmetric bending mode) [18].

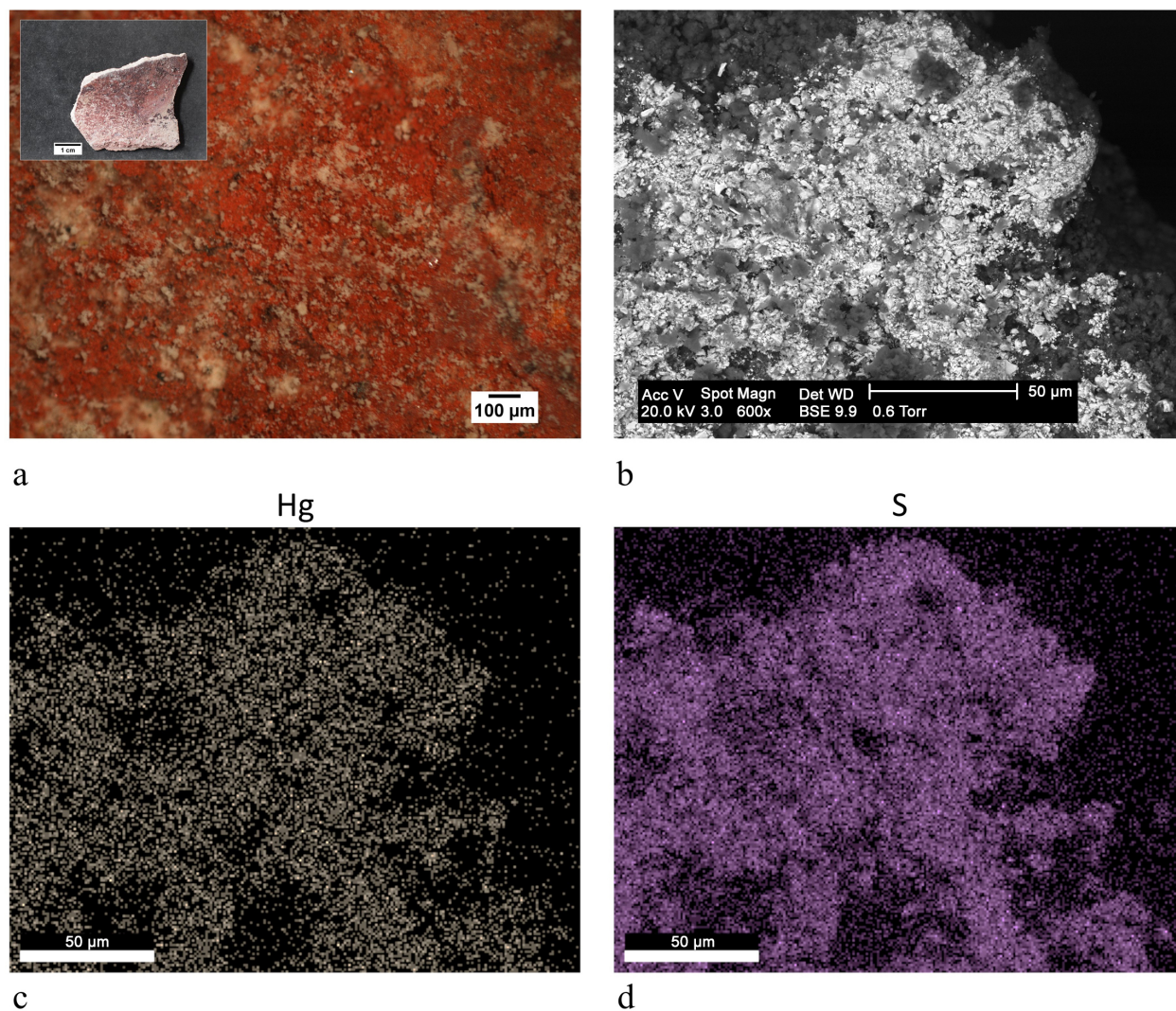


Figure 5. Red area of sample ST15: (a) digital microscope image of the surface (scale bar: $100\ \mu\text{m}$); (b) SEM image in BSE mode of the painted layer (scale bar: $50\ \mu\text{m}$); (c) EDX elemental distribution map of mercury (scale bar: $50\ \mu\text{m}$); (d) EDX elemental distribution maps of sulfur (scale bar: $50\ \mu\text{m}$).

Some samples presented IR patterns (Figure 2d) showing absorbances at around 1645 and 1322 cm^{-1} (C-O stretching vibration) and 668 cm^{-1} (O-C-O bending vibrations), which were ascribed to calcium oxalate ($\text{CaC}_2\text{O}_4 \cdot n\text{H}_2\text{O}$) [18]. The spectra also show the signals at around 2918, 2850 and 1733 cm^{-1} , which suggest the CH and C=O stretching absorption of organic compounds, respectively, but were too weak and few for a reliable identification [7].

In a few green areas, zinc, chlorine and copper appeared to be associated in the EDX maps, as observed in samples ST8 and ST11 (Figures 6 and 7). The combination of these elements suggests the compound $((\text{Cu,Zn})_2(\text{OH})_3\text{Cl})$, known as Brunswick green. XRD analyses of the same samples suggested the presence of the natural equivalent of the pigment, i.e., paratacamite (Figure 6). In sample ST11, Brunswick green was identified in green areas close to yellow areas painted with chrome yellow, as clearly shown in Figure 6.

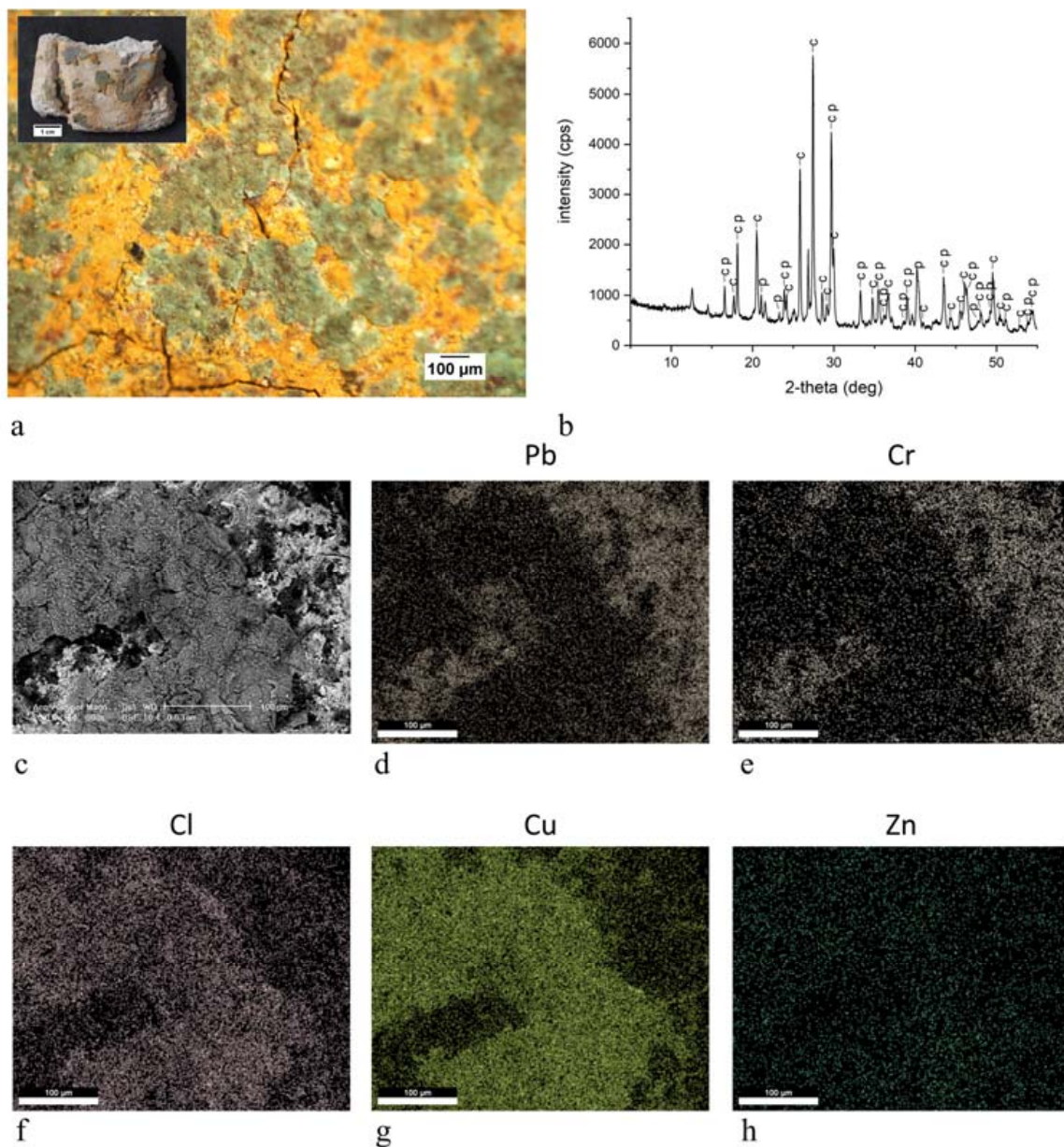


Figure 6. Yellow and green areas of sample ST11: (a) digital microscope image of the surface (scale bar: 100 μm); (b) XRD analysis on powders, showing the main signals of crocoite (c) and paratacamite (p); (c) SEM image in BSE mode of the painted layer (scale bar: 100 μm); (d) EDX elemental distribution maps of lead (scale bar: 100 μm); (e) EDX elemental distribution maps of chromium (scale bar: 100 μm); (f) EDX elemental distribution maps of chlorine (scale bar: 100 μm); (g) EDX elemental distribution maps of copper (scale bar: 100 μm); (h) EDX elemental distribution maps of zinc (scale bar: 100 μm).

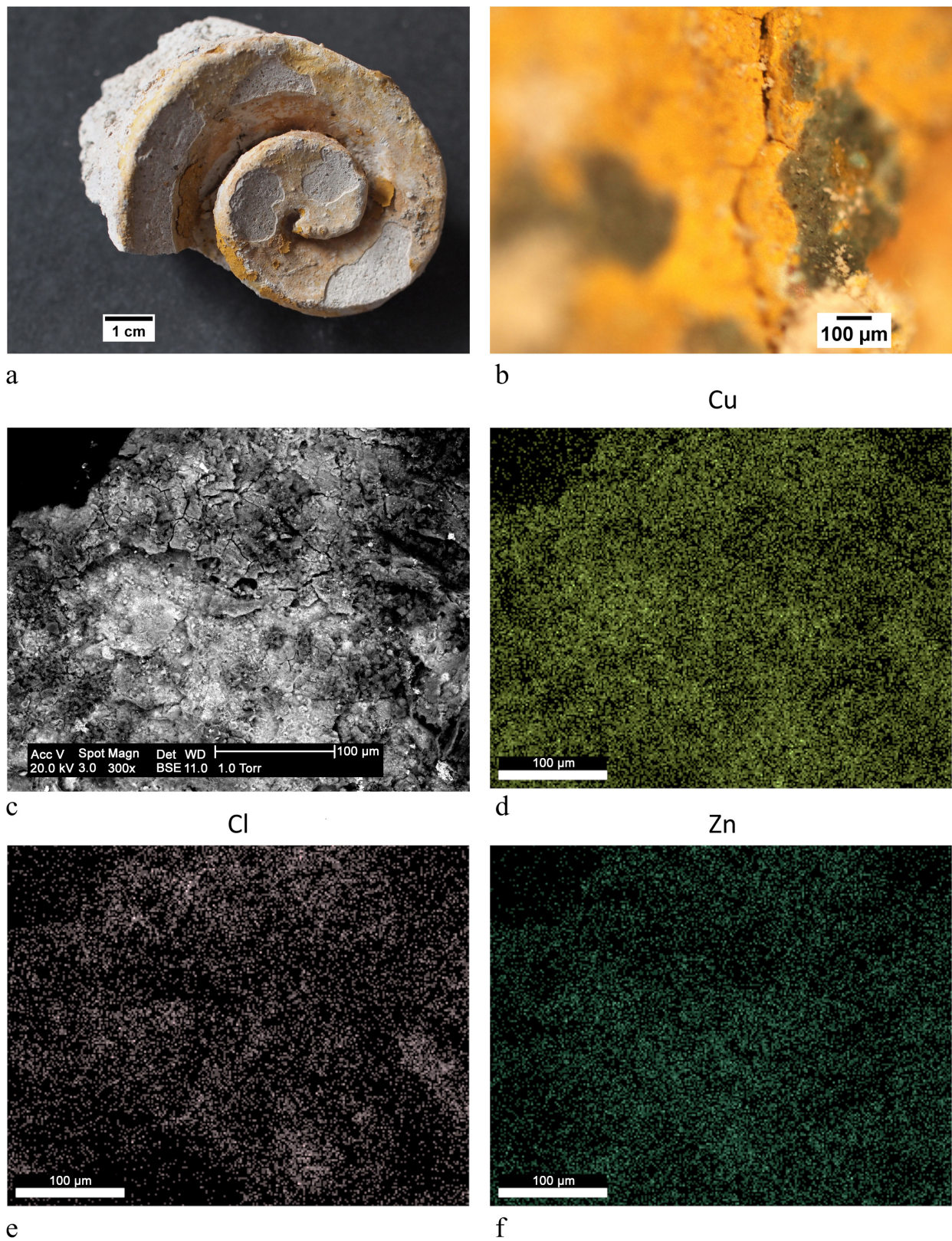


Figure 7. Green area of sample ST8: (a) image of the sample; (b) digital microscope image of details of the green areas of the painted surface (scale bar: 100 μm); (c) SEM image in BSE mode of the painted layer (scale bar: 100 μm); (d) EDX elemental distribution map of copper (scale bar: 100 μm); (e) EDX elemental distribution maps of chlorine (scale bar: 100 μm); (f) EDX elemental distribution maps of zinc (scale bar: 100 μm).

With regards to stratigraphical studies, optical and electronic microscopy revealed a number of colored layers ranging from three to eight. A combination of the EDX elemental maps recorded along the stratigraphy and the IR analysis of the single layers taken, where possible, with micro scalpel, suggested the pigments present in the samples (Table 1). Ochre is the most common pigment, generally alternated with bianco di Sangioanni white and ultramarine blue. In samples ST3 and ST13, the EDX maps recorded the signals of barium and chrome in the same areas (Figure 8). The combination of these two elements resembles the pigment barium chromate called ultramarine yellow or lemon yellow [6]. Analysis of the polished cross sections revealed strange combinations of pigments. Figure 9 shows the stratigraphy of sample ST20. The inner red layer seems to consist of the overlapping of a layer of cinnabar/vermilion and ochre, due to the presence of an accumulation of mercury and iron, respectively. On the other hand, the alternation of only ochre and azurite was observed in sample ST19.

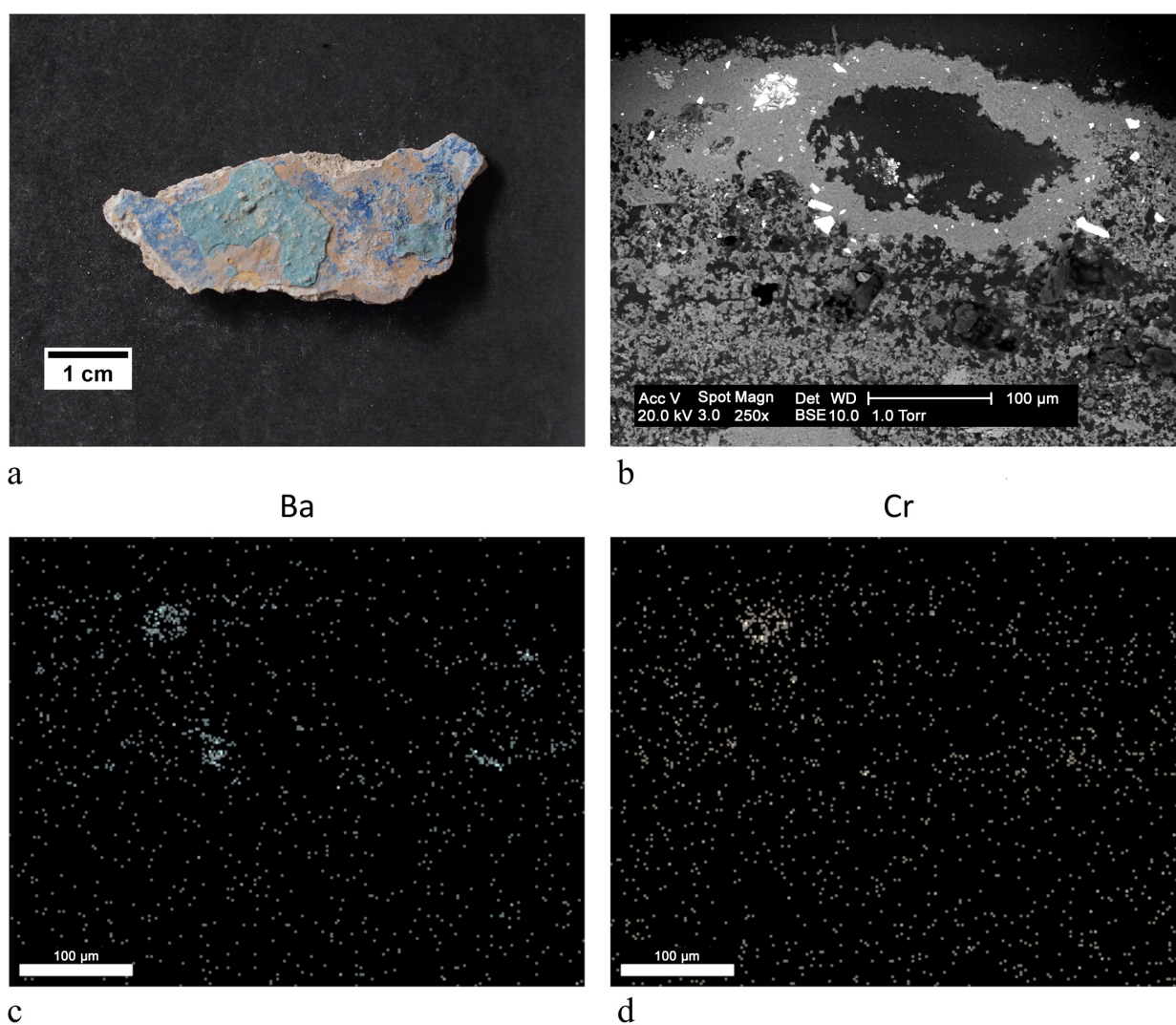


Figure 8. Yellow area of sample ST3: (a) image of the sample; (b) SEM image in BSE mode of the painted layer (scale bar: 100 μm); (c) EDX elemental distribution map of barium (scale bar: 100 μm); (d) EDX elemental distribution maps of chromium (scale bar: 100 μm).

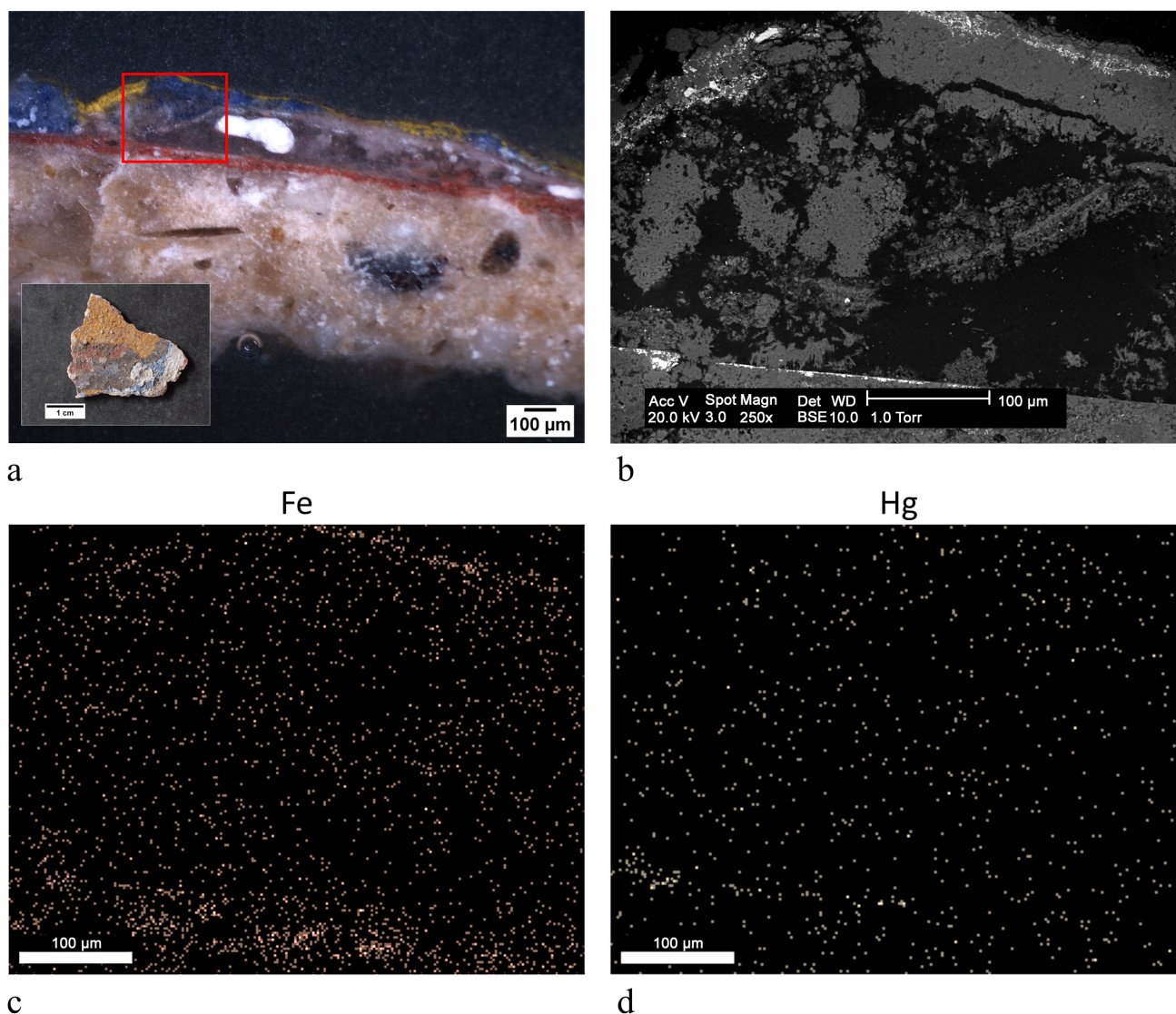


Figure 9. Polished cross section of sample ST20: (a) digital microscope image of the surface (scale bar: 100 µm); (b) SEM image in BSE mode of the painted layer (scale bar: 100 µm). The analyzed area roughly corresponds to the area evidenced in red in the figure (a); (c) EDX elemental distribution map of iron (scale bar: 100 µm); (d) EDX elemental distribution maps of mercury (scale bar: 100 µm).

4. Discussion

The pigments identified are both traditional and modern colors, such as chrome yellow and blanc fixe, above all as an extender, that were first used at the end of the 18th century [16].

Clinochlore was identified in the aqua green area of one sample. This mineral belongs to the chlorite family, which is one of the clay minerals that make up green earths, along with glauconite and celadonite [6]. The presence of only clinochlore for the green color is rare but possible, as documented in two articles [19,20].

In two samples, Brunswick green was found, which is another uncommon pigment. This color was first prepared in the town of Braunschweig (“Brunswick”) in 1764 [6] and was one of the modern pigments that replaced the expensive malachite [21]. It consisted primarily of atacamite; however, a variation of the main recipe included the use of zinc salts to form paratacamite. The occurrence of copper and chlorine also indicates the presence of atacamite, which is also a possible pigment, or maybe the result of the decay of azurite. However, zinc was found in the same areas of the pigment, thus suggesting the presence

of Brunswick green. We ruled out the presence of zinc due to zinc white. In fact, zinc was not found in other areas of the wall paintings. From the beginning of the 19th century, various recipes were developed to produce Brunswick green. However unfortunately the term “Brunswick green” was also applied to colors that referred to other compositions, such as emerald green, verdigris, Prussian blue mixed with chrome yellow and various yellow, brown and black pigments. According to Eastaugh et al. [6], the abundance of meanings suggests that, rather than a specific pigment, Brunswick green was just part of color terminology. The ambiguity of the term and the composition perhaps explain the scarce bibliography of findings of the color in paintings [22,23]. When Brunswick green is mentioned, in fact, the true pigment is misrepresented by a mixture of chrome yellow and Prussian blue. In some cases, the compound may be due to decay phenomena, and thus it is not easy to assess whether the pigment was used as a raw material or whether it was a decay product. In any case, the presence of this pigment also suggests a decorative intervention after the beginning of the 19th century, and therefore following the execution of the first mural paintings.

With regards to the detection of barium chromate, this pigment was commercially available and known throughout the 19th century as ultramarine yellow, lemon yellow, barium yellow, or baryta yellow [6]. It belongs to the family of yellow chromate pigments and has been used since the end of the 19th century, as verified by the finding in paintings of that period [24]. Among chromate pigments, it is the most lightfast and turns green if exposed to light for a long time. Findings of this pigment are also scarce [24–30].

The observation of the stratigraphic sections seems only able to suggest the painting techniques used by the artists. The issue, as emerges also from the literature [31–35], is still very controversial, and, to date, there are no reliable and univocal guidelines. Considering this, microscopic observation seems to suggest a fresco technique for the first decorative cycle, while the finding of organic substances in the outer layers indicates a secco technique for the subsequent interventions.

The presence of gypsum in the majority of samples is likely due to the sulphation of the lime binder fraction, given the poor conditions of the building and the lack of protection from precipitation. The chemical origin of calcium oxalate found in some fragments may be due to the mineralization of organic compounds [36], although films may have been formed as a by-product of surface microflora. SEM morphological investigations did not indicate the presence of either past or present bio-colonization, and traces of organic substances were found in samples containing calcium oxalate. This compound could have formed through the oxidative degradation of the organic binder and/or treatment applied onto the wall painting as part of conservation works.

Our most notable finding was the ubiquitous determination of aragonite, as a component of the supporting mortar. Aragonite is one of the mineralogical forms of calcium carbonate, being of biogenic origin (shells, coral, pearls). When found in the mortar, it is ascribed to the aggregate fraction, as the production of lime, also from the calcination of shells, facilitates the formation of calcite. The most common source of aragonite is from mollusk shells and endoskeleton corals. In some geological formations, it may be associated with specific rocks; however, these rocks are not present in the area of Cerignale.

Dilaria reconstructed in detail the use of aragonite in building technologies [37]. In ancient times, people used shells for food, rituals, decoration, fishing, and for lighting lamps. The shells of some species of *Murex* were also the by-products of the production of purple, an expensive pigment. Once crushed, shells were used as building material, mainly for floors and as an aggregate in mortar. Shells may have been added intentionally in the mixtures to save on the raw materials, and were used as a strong material but, at the same time, were light and therefore easy to transport. Unintentional use cannot be ruled out; for example, when river sands that were not well sieved were used as aggregate. In any case, the use of shells has been described in Roman sources in the 4th century C.E., when it seemed that they improved the set-up of the mixture. Dilaria reports numerous cases of findings in the Mediterranean area, e.g., Greece, Lebanon, Egypt, Italy, Tunisia,

dating from the Bronze Era to the Byzantine Era [37]. Shells have mainly been found in the preparation of floors, wall coverings, foundations of buildings, mosaics, cisterns, but rarely for the mortar support of frescoes. In Italy, shells were used in the north-eastern and central areas, always along the marine coasts and always as building materials for floors and walls. In some cases, it has been possible to trace whether the use is associated with the use of non-sieved sands, in others with the production of purple from the Murex species. It is clear from Dilaria's study that, in every historical period, the use of shells was limited to coastal, lagoon or island territories, since the properties they conferred to mortars were not considered valuable enough to justify their trade.

In most findings on building materials reported in archaeological sources, identification is visual because the shells can still be seen, although partially crushed [37]. Regarding scientific articles on the analytical determination of shells in mortars, aragonite has been revealed by FTIR spectroscopy and XRD in Roman mortars from Caesarea Maritima [38] and in wall paintings exclusively from the Roman and Hellenistic eras [39–44]. Some of these authors have also suggested that aragonite may have been used as a pigment too, alone in white areas or mixed with other pigments, as described in treatises [6].

5. Conclusions

The analysis of the wall paintings of the church of S. Stefano attest to the use of a rich palette of colors and reveal a palimpsest of various painting cycles, as highlighted by the presence of multilayered stratigraphies. Together with common colors, such as ochre, ultramarine blue, bianco di Sangioanni, cinnabar/vermilion, azurite, a few unusual pigments were identified, specifically clinocllore, Brunswick green, ultramarine yellow, which have rarely been found in painted works of art and never in wall paintings. The presence of these pigments datable to the 19th century, indicate a terminus post quem for the execution of the external pictorial layers. Under the microscope, the underlying layers do not appear to be particularly decayed and therefore did not need to be hidden with other colors. This suggests that the building was painted regularly following whatever tastes were current at the time, using synthetic pigments available on the market from the 19th century. Indeed, there are no records on the most recent restoration works and pictorial cycles. Thus, the identification of modern pigments contributes to shedding light on the non-documented history of the monument.

The results unfortunately also reveal, as expected, the dramatic past and present state of conservation of the paintings. Most have come away from the support; however, those that still survive have been covered on the surface by gypsum and calcium oxalate.

Finally, the ubiquitous presence of aragonite due to the intentional use of shells as an aggregate in mortar is particularly interesting. What is surprising is that the literature shows that this is the only case of this finding in wall paintings that are not from the Roman era. This therefore reveals the use of a building technology from the past in this area of the Apennines, perhaps due to its proximity to the Trebbia River and the Ligurian Sea. It is worth highlighting the importance of this area in trade between the Po Valley and Liguria. It was therefore a very frequented area, probably with the exchange of building practices that could have entailed the use of shells in mortars. It would be interesting to investigate other historical buildings in the area of Cerignale, as the discovery elsewhere of aragonite in mortars would corroborate our hypothesis. Shells were probably used as light aggregate and were therefore easy to transport to the church of S. Stefano, which is located far from the main roads and at an altitude of 700 m. The shells may have originated from the Trebbia River, in the valley below, or in the Ligurian sea, to which the Trebbia valley was connected.

The analyses carried out provide evidence of the unexpected richness and variety of the paintings in the church of S. Stefano, which is at real risk of fading. It is thus important to underline the fundamental role of conservation science, which, by studying the techniques and materials used by the artists of the past, may encourage future restoration projects and enhances and preserves the disappearing beauty.

Author Contributions: Conceptualization, L.R.; investigation, C.C., L.G. and L.R.; writing—original draft preparation, C.C. and L.R.; writing—review and editing, C.C., L.G., L.R. and S.R. All authors have read and agreed to the published version of the manuscript.

Funding: This research received no specific grant from any funding agency in the public, commercial or not-for-profit sectors.

Institutional Review Board Statement: Not applicable.

Informed Consent Statement: Not applicable.

Data Availability Statement: The data presented in this study are available on request from the corresponding author.

Acknowledgments: The authors would like to thank Chiara Zannin, Giorgio Castignoli, Giorgio Villa, The Curia Vescovile di Piacenza-Bobbio, The Soprintendenza Archeologia, Belle Arti e Paesaggio per le province di Parma e Piacenza, The Municipality of Cerignale and its mayor Massimo Castelli, The Pro Loco of Cerignale, The Fondazione Banca del Monte di Lombardia and Norberto Masciocchi for support.

Conflicts of Interest: The authors declare no conflict of interest.

References

1. Pearce, M. Reconstructing past transapennine routes: The Trebbia valley. *Reconstr. Past Transapennine Routes Trebbia Val.* **2002**, *6*, 181–183.
2. Wilson, M.J. *Clay Mineralogy: Spectroscopic and Chemical Determinative Methods*; Chapman & Hall: London, UK, 1994; ISBN 9780412533808.
3. Bikiaris, D.; Daniilia, S.; Sotiropoulou, S.; Katsimbiri, O.; Pavlidou, E.; Moutsatsou, A.P.; Chrysoulakis, Y. Ochre-differentiation through micro-Raman and micro-FTIR spectroscopies: Application on wall paintings at Meteora and Mount Athos, Greece. *Spectrochim. Acta Part A Mol. Biomol. Spectrosc.* **2000**, *56*, 3–18. [[CrossRef](#)]
4. Bugini, R.; Corti, C.; Folli, L.; Rampazzi, L. Unveiling the Use of Creta in Roman Plasters: Analysis of Clay Wall Paintings from Brixia (Italy). *Archaeometry* **2017**, *59*, 84–95. [[CrossRef](#)]
5. Crupi, V.; La Russa, M.F.; Venuti, V.; Ruffolo, S.; Ricca, M.; Paladini, G.; Albin, R.; Macchia, A.; Denaro, L.; Birarda, G.; et al. A combined SR-based Raman and InfraRed investigation of pigments used in wall paintings: The San Gennaro and San Gaudioso Catacombs (Naples, Italy) case. *Eur. Phys. J. Plus* **2018**, *133*, 369. [[CrossRef](#)]
6. Eastaugh, N.; Walsh, V.; Chaplin, T.; Siddall, R. *Pigment Compendium: A Dictionary and Optical Microscopy of Historical Pigments*; Pigment Compendium: A Dictionary and Optical Microscopy of Historical Pigments; Butterworth-Heinemann: Oxford, UK, 2008; ISBN 9780750689809.
7. Derrick, M.R.; Stulik, D.; Landry, J.M. *Infrared Spectroscopy in Conservation Science*; The Getty Conservation Institute: Los Angeles, CA, USA, 1999; ISBN 0892364696.
8. Bugini, R.; Corti, C.; Folli, L.; Rampazzi, L. Roman Wall Paintings: Characterisation of Plaster Coats Made of Clay Mud. *Heritage* **2021**, *4*, 48. [[CrossRef](#)]
9. Montoya, C.; Lanas, J.; Arandigoyen, M.; Navarro, I.; García Casado, P.J.; Alvarez, J.I. Study of ancient dolomitic mortars of the church of Santa Maria de Zamarce in Navarra (Spain): Comparison with simulated standards. *Thermochim. Acta* **2003**, *398*, 107–122. [[CrossRef](#)]
10. Igea, J.; Lapuente, P.; Martínez-Ramírez, S.; Blanco-Varela, M.T. Characterization of mudejar mortars from St. Gil Abbot church (Zaragoza, Spain): Investigation of the manufacturing technology of ancient gypsum mortars. *Mater. Constr.* **2012**, *62*, 515–529. [[CrossRef](#)]
11. Biscontin, G.; Pellizon Birelli, M.; Zendri, E. Characterization of binders employed in the manufacture of Venetian historical mortars. *J. Cult. Herit.* **2002**, *3*, 31–37. [[CrossRef](#)]
12. Crupi, V.; D'Amico, S.; Denaro, L.; Donato, P.; Majolino, D.; Paladini, G.; Persico, R.; Saccone, M.; Sansotta, C.; Spagnolo, G.V.; et al. Mobile Spectroscopy in Archaeometry: Some Case Study. *J. Spectrosc.* **2018**, *2018*, 1–11. [[CrossRef](#)]
13. Zhang, K.; Grimoldi, A.; Rampazzi, L.; Sansonetti, A.; Corti, C. Contribution of thermal analysis in the characterization of lime-based mortars with oxblood addition. *Thermochim. Acta* **2019**, *678*, 178303. [[CrossRef](#)]
14. Zhang, K.; Corti, C.; Grimoldi, A.; Rampazzi, L.; Sansonetti, A. Application of Different Fourier Transform Infrared (FT-IR) Methods in the Characterization of Lime-Based Mortars with Oxblood. *Appl. Spectrosc.* **2019**, *73*, 479–491. [[CrossRef](#)]
15. Žigovečki Gobac, Ž.; Posilović, H.; Bermanec, V. Identification of biogenetic calcite and aragonite using SEM. *Geol. Croat.* **2009**, *62*, 201–206. [[CrossRef](#)]
16. Roy, A. *Artists' Pigments: A Handbook of Their History and Characteristics*; Oxford University Press: London, UK, 1993; Volume 2, ISBN 9780894681899.
17. Aroke, U.O.; Abdulkarim, A.; Ogubunka, R.O. Fourier-transform Infrared Characterization of Kaolin, Granite, Bentonite and Barite. *ATBU J. Environ. Technol.* **2013**, *6*, 42–53.

18. Ranalli, G.; Bosch-Roig, P.; Crudele, S.; Rampazzi, L.; Corti, C.; Zanardini, E. Dry biocleaning of artwork: An innovative methodology for Cultural Heritage recovery? *Microb. Cell* **2021**, *8*, 91–105. [[CrossRef](#)]
19. Edreira, M.C.; Feliu, M.J.; Fernández-Lorenzo, C.; Martín, J. Roman wall paintings characterization from Cripta del Museo and Alcazaba in Mérida (Spain): Chromatic, energy dispersive X-ray fluorescence spectroscopic, X-ray diffraction and Fourier transform infrared spectroscopic analysis. *Anal. Chim. Acta* **2001**, *434*, 331–345. [[CrossRef](#)]
20. Gebremariam, K.F.; Kvittingen, L.; Banica, F.-G. Physico-Chemical Characterization of Pigments and Binders of Murals in a Church in Ethiopia. *Archaeometry* **2016**, *58*, 271–283. [[CrossRef](#)]
21. Scott, D.A. *Copper and Bronze in Art: Corrosion, Colorants, Conservation*; Getty Conservation Institute: Los Angeles, CA, USA, 2002; ISBN 0892366389.
22. Setti, M.; Lanfranchi, A.; Cultrone, G.; Marinoni, L. Archaeometric investigation and evaluation of the decay of ceramic materials from the church of Santa Maria del Carmine in Pavia, Italy. *Mater. Constr.* **2012**, *62*, 79–98. [[CrossRef](#)]
23. Gabrielli, N. Technical-scientific investigations to detect the temporal vicissitudes of the funeral monument of Innocent VIII (Giovannibattista Cibo, 1484–1492), compared with that of Sixtus IV (Francesco della Rovere 1471–1484), both made by Antonio del Pollaiuolo. *Nat. Prod. Res.* **2019**, *33*, 926–936. [[CrossRef](#)]
24. Otero, V.; Campos, M.F.; Pinto, J.V.; Vilarigues, M.; Carlyle, L.; Melo, M.J. Barium, zinc and strontium yellows in late 19th–early 20th century oil paintings. *Herit. Sci.* **2017**, *5*, 46. [[CrossRef](#)]
25. Fulton, E.L.; Newman, R.; Woodward, J.; Wright, J. The Methods and Materials of Martin Johnson Heade. *J. Am. Inst. Conserv.* **2002**, *41*, 155. [[CrossRef](#)]
26. Klyachkovskaya, E.V.; Kozhukh, N.M.; Rozantsev, V.A.; Gaponenko, S.V. Layer-by-Layer Laser Spectrum Microanalysis of Easel-Painting Materials. *J. Appl. Spectrosc.* **2005**, *72*, 371–375. [[CrossRef](#)]
27. Vetter, W.; Schreiner, M. A Fiber Optic Reflection-UV/Vis/NIR-System for Non-Destructive Analysis of Art Objects. *Adv. Chem. Sci.* **2014**, *3*, 7–14.
28. Grifoni, E.; Briganti, L.; Marras, L.; Orsini, S.; Colombini, M.P.; Legnaioli, S.; Lezzerini, M.; Lorenzetti, G.; Pagnotta, S.; Palleschi, V. The chemical-physical knowledge before the restoration: The case of “The Plague in Lucca”, a masterpiece of Lorenzo Viani (1882–1936). *Herit. Sci.* **2015**, *3*, 26. [[CrossRef](#)]
29. Romano, F.P.; Caliri, C.; Nicotra, P.; Di Martino, S.; Pappalardo, L.; Rizzo, F.; Santos, H.C. Real-time elemental imaging of large dimension paintings with a novel mobile macro X-ray fluorescence (MA-XRF) scanning technique. *J. Anal. At. Spectrom.* **2017**, *32*, 773–781. [[CrossRef](#)]
30. Cristea-Stan, D.; Constantinescu, B. Studies on pigments of religious mural paintings using a portable X-ray Fluorescence spectrometer—The cases of Urechesi-Cicanesti Arges and Icoanei Bucuresti churches. *Proc. Rom. Acad. Ser. A* **2019**, *20*, 347–352.
31. Regazzoni, L.; Cavallo, G.; Biondelli, D.; Gilardi, J. Microscopic Analysis of Wall Painting Techniques: Laboratory Replicas and Romanesque Case Studies in Southern Switzerland. *Stud. Conserv.* **2018**, *63*, 326–341. [[CrossRef](#)]
32. Kriznar, A.; Ruiz-Conde, A.; Sánchez-Soto, P.J. Microanalysis of Gothic mural paintings (15th century) in Slovenia: Investigation of the technique used by the Masters. *X-ray Spectrom.* **2008**, *37*, 360–369. [[CrossRef](#)]
33. Piovesan, R.; Mazzoli, C.; Maritan, L.; Cornale, P. Fresco and lime-paint: An experimental study and objective criteria for distinguishing between these painting techniques. *Archaeometry* **2012**, *54*, 723–736. [[CrossRef](#)]
34. Mugnaini, S.; Bagnoli, A.; Bensi, P.; Droghini, F.; Scala, A.; Guasparri, G. Thirteenth century wall paintings under the Siena Cathedral (Italy). Mineralogical and petrographic study of materials, painting techniques and state of conservation. *J. Cult. Herit.* **2006**, *7*, 171–185. [[CrossRef](#)]
35. Mora, P.; Mora, L.; Philippot, P. *La Conservazione delle Pitture Murali*; Editrice Compositori: Bologna, Italy, 1999; ISBN 8877941839.
36. Rampazzi, L. Calcium oxalate films on works of art: A review. *J. Cult. Herit.* **2019**, *40*, 195–214. [[CrossRef](#)]
37. Dilaria, S. Costruire ingegnosamente riutilizzando materiali poveri. L’impiego di conchiglie a fini edilizi ad Aquileia tra età repubblicana e tarda antichità. *REUDAR. Eur. J. Rom. Archit.* **2017**, *1*, 25. [[CrossRef](#)]
38. Asscher, Y.; van Zuiden, A.; Elimelech, C.; Gendelman, P.; Ad, U.; Sharvit, J.; Secco, M.; Ricci, G.; Artioli, G. Prescreening Hydraulic Lime-Binders for Disordered Calcite in Caesarea Maritima: Characterizing the Chemical Environment Using FTIR. *Radiocarbon* **2020**, *62*, 527–543. [[CrossRef](#)]
39. Brysbaert, A. Lapis Lazuli in an Enigmatic ‘Purple’ Pigment from a Thirteenth-Century BC Greek Wall Painting. *Stud. Conserv.* **2006**, *51*, 252–266. [[CrossRef](#)]
40. Mazzocchin, G.; Del Favero, M.; Tasca, G. Analysis of Pigments from Roman Wall Paintings Found in the “Agro Centuriato” of Julia Concordia (Italy). *Ann. Chim.* **2007**, *97*, 905–913. [[CrossRef](#)]
41. Mazzocchin, G.A.; Vianello, A.; Minghelli, S.; Rudello, D. Analysis of roman wall paintings from the thermae of ‘Iulia Concordia’. *Archaeometry* **2010**, *52*, 644–655. [[CrossRef](#)]
42. Duran, A.; Jimenez De Haro, M.C.; Perez-Rodriguez, J.L.; Franquelo, M.L.; Herrera, L.K.; Justo, A. Determination of pigments and binders in pompeian wall paintings using synchrotron radiation—High-resolution X-ray powder diffraction and conventional spectroscopy—Chromatography. *Archaeometry* **2010**, *52*, 286–307. [[CrossRef](#)]
43. Corti, C.; Rampazzi, L.; Visoná, P. Hellenistic mortar and plaster from Contrada Mella near Oppido Mamertina (Calabria, Italy). *Int. J. Conserv. Sci.* **2016**, *7*, 57–70.
44. Garofano, I.; Perez-Rodriguez, J.L.; Robador, M.D.; Duran, A. An innovative combination of non-invasive UV-Visible-FORS, XRD and XRF techniques to study Roman wall paintings from Seville, Spain. *J. Cult. Herit.* **2016**, *22*, 1028–1039. [[CrossRef](#)]